ELSEVIER

International Journal of Heat and Fluid Flow 19 (1998) 320–325

International Journal of HEAT AND FLUID FLOW

Direct numerical simulation of transition in pipe flow under the influence of wall disturbances

H. Shan [a], Z. Zhang [a], F.T.M. Nieuwstadt [b,*]

[a] Department of Engineering and Mechanics, Tsinghua University, 100084 Beijing, People's Republic of China
[b] J.M. Burgers Centre, Delft University of Technology, Mechanical Engineering and Marine Technology, Rotterdamseweg 145, 2628 AL Delft, The Netherlands

Received 12 July 1997; accepted 28 March 1998

Abstract

In this paper we consider a direct numerical simulation of transition from laminar to turbulent flow excited by wall disturbances in a cylindrical pipe. The wall disturbances are imposed by means of blowing and suction through the pipe wall. Two cases are considered: periodic suction/blowing (PSB) and random suction/blowing (RSB). The former case can be interpreted as a pipe flow in combination with a periodic roughness element of a fixed size and the latter as a pipe with randomly distributed wall roughness elements. For the PSB case the critical amplitude of the blowing/suction velocity that causes transition is obtained. The dependence of this critical amplitudes on the Reynolds number is considered. In addition the dependence of the transition time on the suction/blowing amplitudes and the Reynolds number is investigated. This latter parameter is also considered for the RSB case.

Keywords: Pipe flow; Direct numerical simulation; Roughness; Transition

Notation

A_w	amplitude of radial disturbance velocity non-dimensionalized with U_B
D	pipe diameter $= 2R$
E	total kinetic energy of the flow
$E(n, m)$	kinetic energy of mode (n, m)
m	wavenumber in the azimuthal direction
n	wavenumber in the axial direction
p	static pressure
P	total pressure
r	radial coordinate non-dimensionalized with pipe radius R
R	pipe radius
Re	Reynolds number $(U_B R/\nu)$
Re_D	Reynolds number $(U_B D/\nu)$
u	axial velocity component non-dimensionalized with U_B
u_τ	friction velocity
U_B	bulk velocity
v	tangential velocity component non-dimensionalized with U_B
$\boldsymbol{v}$	velocity vector
w	radial velocity component non-dimensionalized with U_B
x	axial coordinate non-dimensionalized with pipe radius R
X	pipe length
α	$2\pi R/X$
θ	tangential coordinate
ν	kinematic viscosity
$\boldsymbol{\omega}$	vorticity

1. Introduction

The study of transition from laminar to turbulent flow in a smooth circular pipe can be traced back to the famous experiment carried out by Reynolds in 1883. Since then progress in the research on the stability of pipe flow has been slow. The main reason for this is the fact that the standard strategy to investigate the stability of a flow, i.e. linear stability theory, fails in this case. Namely, all infinitesimal perturbations superposed on the laminar Poiseuille profile have been found to decay (Gill, 1965; Lessen et al., 1968; Salwen et al., 1980). This means that to study transition in pipe flow one has to consider finite disturbances or alternatively non-linear theory. Some attempts to consider transition theoretically have been made, such as weakly non-linear theory (Davey and Nguyen, 1971; Patera and Orszag, 1981), the theory of non-linear critical layers (Smith and Bodonyi, 1982) and transient growth (Trefethen et al., 1993; O'Sullivan and Breuer, 1994a, b). However, the problem of transition in pipe flow must be still considered as open.

* Corresponding author. E-mail: f.nieuwstadt@wbmt.tudelft.nl.

0142-727X/98/$19.00
PII: S0142-727X(98)10008-5

Above we have referred to the transition in a smooth pipe. In the present study we consider the transition process under the influence of wall disturbances such as roughness elements. It is generally believed that wall roughness promotes transition but the details of the transition process are again not known. Analysis of transition by means of theoretical methods seems much more difficult in this case and we therefore turn to a direct numerical simulation (DNS) as an alternative approach to study transition in rough-walled pipes.

The objective of the present work is to investigate the influence of regular and irregular distributed wall disturbances on the transition of laminar flow in a circular pipe. The disturbances are applied as blowing and suction through the wall of the pipe. The blowing/suction will displace the laminar pipe flow in the wall-normal direction and therefore its effect can be interpreted to a first approximation as that of a roughness element. The distribution of blowing and suction then determines the distribution of wall-roughness elements. Two cases will be distinguished: Periodic Suction/Blowing (PSB) which gives a regular roughness distribution and Random Suction/Blowing (RSB) which is taken to be representative for a fully rough pipe with randomly distributed roughness elements.

To give an outline of the paper we will first discuss the numerical methods that we have used. Next we consider the results of our simulations. First, the results of the PSB case for an axisymmetric and non-axisymmetric disturbance pattern, will be presented. Second, the results of the RSB case for a random disturbance patterns are discussed. We end with some conclusions.

2. Numerical methods

The problem that we consider is governed by the Navier–Stokes equations for a incompressible flow. These equations can be written as

$$\frac{\partial \boldsymbol{v}}{\partial t} + \boldsymbol{\omega} \times \boldsymbol{v} = -\nabla P + \frac{1}{\mathrm{Re}} \nabla^2 \boldsymbol{v} \tag{1}$$

for conservation of momentum and

$$\nabla \cdot \boldsymbol{v} = 0 \tag{2}$$

for the conservation of mass. In these equations $P = p + |\boldsymbol{v}|^2/2$ denotes the total pressure, $\boldsymbol{v}$ the velocity field and $\boldsymbol{\omega} = \nabla \times \boldsymbol{v}$ is the vorticity. The equations have been non-dimensionalized with help of a characteristic length, velocity and time scale which in this case are chosen to be the pipe radius R, the bulk velocity U_B and R/U_B, respectively. With these scales we can define the Reynolds number $\mathrm{Re} = U_\mathrm{B} R/v$. The solution of these equation for the case of a pipe geometry is most conveniently expressed in a cylindrical coordinate system where x, θ, r stand for the axial, azimuthal and radial direction. The velocity components in the three directions are denoted by u, v, w, respectively.

The computational domain and the cylindrical coordinate system is illustrated in Fig. 1. In this domain the equations of motion (1) and (2) are solved numerically by means of a spectral element method based on an expansion in Fourier functions and Chebyshev polynomials. The flow conditions in the azimuthal direction are periodic by definition. We also apply the condition of periodicity in the axial direction which implies that only flow disturbances with a length scale less than $X/2$ can be represented. In both periodic directions a Fourier expansion for the total pressure and velocity has been adopted given by

$$P(r,\theta,x) = \sum_{m=-M/2}^{m=M/2-1} \sum_{n=-N/2}^{n=N/2-1} \hat{P}(r,m,n) \mathrm{e}^{\mathrm{i}(n\alpha x + m\theta)}, \tag{3}$$

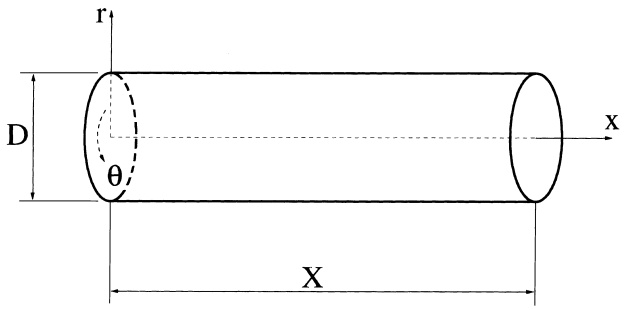

Fig. 1. Computational domain in a cylindrical coordinate system.

$$\boldsymbol{v}(r,\theta,x) = \sum_{m=-M/2}^{m=M/2-1} \sum_{n=-N/2}^{n=N/2-1} \hat{\boldsymbol{v}}(r,m,n) \mathrm{e}^{\mathrm{i}(n\alpha x + m\theta)}, \tag{4}$$

where $\alpha = 2\pi R/X$ and where n and m denote the wave numbers in the axial and azimuthal direction, respectively. In the radial direction, a spectral element method based on a domain decomposition technique is used. The radial domain is subdivided into several ring-shaped elements and a cylindrical element in the centre. The boundary of each element is determined by

$$r_i = (1 - r_\mathrm{c}) \left\{ \ln \left[\frac{N_\mathrm{e} - i}{N_\mathrm{e} - 1} (e - 1) + 1 \right] \right\}^{1/2} + r_\mathrm{c}, \tag{5}$$

where $i = 1, 2, \ldots, N_\mathrm{e}$ are the indices of the elements counted from the wall and r_c is the size of the central element. In our case r_c has been taken equal to $0.1R$. The non-central ring-shaped elements gradually increase in size going from the wall to the centre region of the pipe.

Each element is mapped onto interval $[-1, 1]$ by means of a linear transformation. In the ith element, i.e. the domain for which $r \in [r_{i+1}, r_i]$ a local coordinate $y^i \in [-1, 1]$ is defined according to

$$y^i = 2 \frac{r - r_{i+1}}{r_i - r_{i+1}} - 1.$$

Inside each element, a set of Chebyshev–Gauss–Lobatto collocation points is defined with the value of the local coordinates given by

$$y_k^i = \cos \frac{\pi k}{N_P^i},$$

where i denotes the ith element and where $k = 0, 1, 2, \ldots, N_i^P$ with N_i^P the total number of collocation points in the ith element. There is a common collocation point for the adjacent elements.

To solve the Eqs. (1) and (2) we employ a time splitting method in which the non-linear, the pressure gradient and the viscous terms are integrated sequentially. The so-called stiffly stable scheme (Karniadakis et al., 1991) is applied in three steps as follows:

The first sub-step: Integration of non-linear term

$$\frac{\boldsymbol{v}^{n+1/3} - \sum_{q=0}^{J_\mathrm{i}-1} \alpha_q \boldsymbol{v}^{n-q}}{\Delta t} = \sum_{q=0}^{J_\mathrm{e}-1} \beta_q (\boldsymbol{v} \times \boldsymbol{\omega})^{n-q} - \frac{\mathrm{d}\bar{p}}{\mathrm{d}x} \mathrm{e}_x, \tag{6}$$

where $\mathrm{d}\bar{p}/\mathrm{d}x$ is the average axial pressure gradient. The $J_\mathrm{e} = J_i = 3$, with coefficients $\alpha_0 = 3$, $\alpha_1 = -3/2$, $\alpha_2 = 1/3$, $\beta_0 = 3$, $\beta_1 = -3$, $\beta_2 = 1$, which corresponds to a 3rd-order time accurate scheme.

The second sub-step: Integration of pressure gradient

$$\frac{\boldsymbol{v}^{n+2/3} - \boldsymbol{v}^{n+1/3}}{\Delta t} = -\nabla P^{n+1}, \tag{7}$$

where continuity is imposed by setting

$$\nabla \cdot \boldsymbol{v}^{n+2/3} = 0. \tag{8}$$

As a result we obtain a Poisson equation for the total pressure which reads

$$\nabla^2 P^{n+1} = \frac{1}{\Delta t} \nabla \cdot \boldsymbol{v}^{n+1/3}. \tag{9}$$

The third sub-step: Integration of viscous term

$$\frac{\gamma_0 \boldsymbol{v}^{n+1} - \boldsymbol{v}^{n+2/3}}{\Delta t} = \frac{1}{\mathrm{Re}} \nabla^2 \boldsymbol{v}^{n+1}, \tag{10}$$

where $\gamma_0 = 11/6$.

The time step Δt is taken in all our computations equal to $0.01R/U_B$.

As initial condition we start from a fully developed Poiseuille profile for a laminar pipe flow. At time $t = 0$ perturbations are imposed on this flow in the form of a given radial velocity at the pipe wall in the form of suction and blowing. In all cases, the total net flux due to the suction/blowing through the wall is maintained equal to zero. The first effect of suction/blowing is to displace the axial flow in the radial direction and this may be taken as equivalent to the influence on the flow by a wall roughness element. Several distributions of the wall suction/blowing are considered and these can by distinguished into two categories.

The first category is so-called periodic-suction/blowing (PSB) by which a pipe wall is simulated with regularly distributed roughness elements of a single size. In this category two cases are considered:

(a) *Axisymmetrically distributed disturbance:* In this case the normal velocity on the pipe wall is prescribed following:

$$w_{\mathrm{dis}}(\theta, x) = A_{\mathrm{w}} \sin(k_x \alpha x), \tag{11}$$

where A_{w} is the amplitude of the radial velocity and k_x the axial wave number of the velocity disturbance which is representative for the size of the roughness element. We note again that both A_{w} and k_x have been made dimensionless with the bulk velocity U_B and the pipe radius R as characteristic velocity and length scale.

(b) *Non-axisymmetrically distributed disturbance:* The wall-normal velocity in this case is given by

$$w_{\mathrm{dis}}(\theta, x) = A_{\mathrm{w}} \sin(k_x x) \cos(k_\theta \theta), \tag{12}$$

where A_{w} is again the amplitude and the k_x and k_θ are the axial and the azimuthal wave number, respectively. In this case the roughness distribution has a helical pattern.

The second category is random-suction/blowing (RSB) by which a pipe wall is simulated with irregularly distributed roughness elements of varying size. This case is assumed to be representative for a fully rough pipe wall.

(c) *Randomly distributed disturbance:* The wall normal velocity is for this case prescribed according to

$$w_{\mathrm{dis}}(\theta, x) = \mathrm{Rand}(\theta, x), \tag{13}$$

where $\mathrm{Rand}(\theta, x)$ is a random field over the $x - \theta$ plane with an uniform probability density. The mean value of this random field is zero and its root-mean-square value is denoted as A_{rms}.

In our computations to be presented in the following sections, we have taken the (non-dimensional) length X of the pipe equal to 2π. In the spectral element method we have taken the number of (ring-shaped) elements equal to 4 with each 16 collocation points except the central cylindrical element which has only four points. Thus, the total number of collocation points in the radial direction is 53. The number of Fourier modes in the tangential direction that we have used, varies between 8 for the PSB case and 32 for the RSB case. The number of grid points in the axial direction is 32.

The domain length of $2\pi R$ may be considered as too small and the maximum resolution of $53 \times 32 \times 32$ as too low for a DNS of turbulent pipe flow at the Reynolds numbers that we consider here (Eggels et al., 1994). However, we stress that we do not aim to compute a fully developed turbulent pipe flow in this study but rather the start of transition from laminar to turbulent flow in this geometry. The initial phase of such transition process is usually dominated by large-scale disturbance in the flow, say of the order of the pipe radius, and these can be adequately resolved by the our computational grid. The intensity of these large-scale disturbance scales grows due to instability and eventually they break-up into smaller scales after which turbulent flow is assumed to develop. Here, we only consider the flow development up to this break-up event, which can be recognized in our computation as a fast growth of energy at all flow scales and which we shall denote as the transition point. After this transition point is reached the computation is stopped.

The advantage of the small resolution that we have adopted here, is that it allows us to perform computations for an extensive range of disturbance parameters. At a larger resolution this would have been prohibitive in terms of computational costs.

3. Results

The results of our computations will be described in the following subsections arranged according to the various disturbance profiles that we have introduced above. For the PSB case we shall limit our computations to a single value of k_x, i.e. $k_x = 4$. Apart from computational limitation, we have chosen for this single value of k_x for the following reasons. A value of $k_x = 4$ means in our case a roughness element with a size of $\mathrm{O}(D)$. This is a disturbance which we can resolve well with our numerical grid where for the case of 32 collocation points in the axial direction the resolution is $\sim 0.2D$. At the same time the intermediate size of our disturbance in terms of the resolution allows (non-linear) interaction with higher harmonics but also with subharmonics and both may play a role in the transition process. We shall see in the following subsection that these two interactions indeed occur. For this reason alternatives for $k_x = 4$ are quite limited and we expect that a slight change of k_x to another value close to 4 would not change the results to be presented in the following very much. In other words, a study of the influence of k_x requires a much higher resolution then the one that we have used here.

3.1. Axisymmetric disturbance distribution

A computation has been carried out with Eq. (11) for the suction/blowing distribution with an amplitude $A_{\mathrm{w}} = 0.1$ (and $k_x = 4$). By means of this disturbance profile we simulate an axisymmetrically distributed wall-roughness element. Despite the fact that this disturbance amplitude $A_{\mathrm{w}} = 0.1$ can be considered as large (we will see in the following sections that for this disturbance amplitude always transition is found when other disturbance distributions are used), no transition is found at the Reynolds numbers, $\mathrm{Re_D} = 3000$ and 5000, for which computations have been carried out. Here, $\mathrm{Re_D}$ denotes the Reynolds number based on the pipe diameter D and the bulk velocity U_B.

It seems that the axisymmetrically roughness elements only excite the axisymmetric modes of the flow which are very stable. In other words the cylindrical pipe flow (at the Reynolds numbers that we consider) is stable to large axisymmetric disturbances. This agrees with the theoretical results of Davey and Drazin (1969).

3.2. Non-axisymmetric disturbance distribution

The non-axisymmetrically distributed wall roughness elements are simulated according to Eq. (12) with an azimuthal wave number $k_\theta = 1$ (the axial wave number of the disturbance is again chosen to be $k_x = 4$). The choice for $k_\theta = 1$ is based on the fact that for this values the least stable eigenmode for infinitesimal perturbations is found. For the amplitude of the suction/blowing we have considered a range of values with $A_w = 0.01 - 0.1U_B$. The Reynolds numbers that we consider are Re_D equal to 2000, 3000, 4000 and 5000.

For the case of $Re_D = 5000$ and $A_w = 0.05$ we show in Fig. 2 wall shear stress averaged over the pipe wall as a function of time. For a laminar flow this non-dimensional wall shear stress is given by

$$\frac{\tau_w}{\rho U_b^2} = \frac{8}{Re_D}. \tag{14}$$

We see that initially the shear stress stays equal to its laminar value. At about $t = 30$ the shear stress departs from this value and starts to grow. The shear stress then reaches a maximum value at $t \simeq 100$ after which the wall-shear stress fluctuates around a value of ~ 0.0045. The flow may then be considered as turbulent. The time interval to the first maximum of the shear stress will be denoted in the following as the transition time.

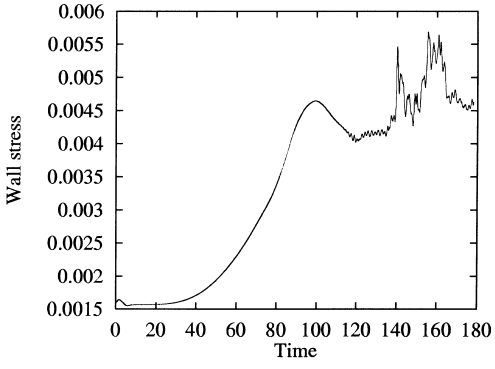

Fig. 2. Wall stress vs. time for the case of the non-axisymmetric roughness element distribution at $Re_D = 5000$, $A_w = 0.05$, $k_x = 4$, $k_\theta = 1$.

The shear stress in Fig. 2 appears to grow rather gradually and this may seem in contradiction with the sudden transition to turbulence which one would expect based on experimental visualization studies. To study the transition process and its time development in more detail we introduce $E(n, m)$ which is defined as

$$E(n,m) = \frac{4\pi^2}{\alpha}\int_0^1 \hat{\mathbf{v}}'(r,n,m)\hat{\mathbf{v}}'_*(r,n,m)r\,\mathrm{d}r, \tag{15}$$

where the index $*$ denotes the complex conjugate and where the prime denotes the deviation of the velocity from laminar Poiseuille profile so that $E(n, m) = 0$ at $t = 0$ for all n and m. The interpretation of $E(n, m)$ is the volume integrated non-dimensional disturbance energy per axial mode n and tangential mode m.

In Fig. 3 we show the time development of various modes $E(n, m)$ given by Eq. (15). It follows that mode (4,1), (4,−1) which is directly excited by the wall disturbance, is constant as a result of the forcing. The energy of this (4,1), (4,−1) mode is transmitted by non-linear interaction to both lower and higher-order modes. In particular the mode (0,2), (0,−2) seems to benefit and it grows gradually starting at $t = 0$ to a large value which stays constant until transition occurs. This mode which as $n = 0$ is independent of the streamwise coordinate, may perhaps be related to the streamwise vortices which have been observed in other studies on the transition of cylindrical pipe flow (Bandyopadhyah, 1986; Shan et al., 1998). With respect to the other modes and in particular with respect to the modes (12,1), (12,−1) and (12,3), (12,−3), we find that the energy of these modes stays small until $t \simeq 250$ and then starts to grow very fast. As these latter modes represent small scale fluctuations, this sudden growth around $t \simeq 250$ may perhaps be identified with the appearance of small scale turbulent fluctuations. This means that also our computations indicate that turbulence appears quite suddenly.

To investigate the transition at various Reynolds number and for various disturbance amplitudes, we have carried out extensive computations. From analysis of the results we have obtained the critical amplitude A_w^* for each Reynolds number which is defined as the value of the wall disturbance amplitude at which transition is first detected. The results for the various calculations together with the critical amplitude are displayed in Fig. 4. The cases where the flow remains stable have been indicated by solid dots and the cases where transition happens

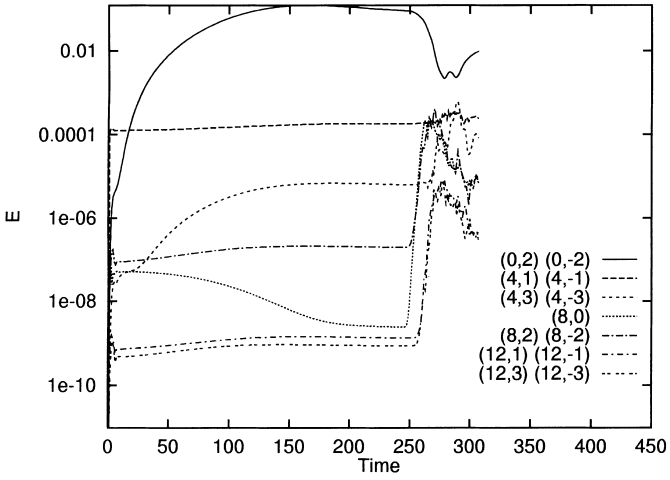

Fig. 3. The non-dimensional disturbance energy $E(n, m)$ for various values of the axial mode (n) and azimuthal mode (m) as a function of time for $Re_D = 3000$, $A_w = 0.03$, $k_x = 4$, $k_\theta = 1$; note that mode (4,1) and (4,−1) has the same axial and azimuthal dependence as the wall disturbance.

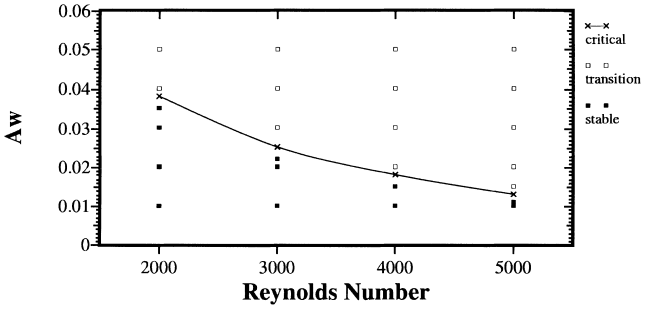

Fig. 4. Amplitude A_w vs. Reynolds number Re_D for the non-axisymmetric disturbance distribution with $k_x = 4$ and $k_\theta = 1$; open markers indicate that transition has been detected and closed markers that the flow remains stable; the solid line gives the critical amplitude A^*.

by open dots, respectively. The critical amplitudes A_w^* are marked by crosses which are connected by a solid line.

Although the range of Reynolds numbers over which A_w^* is computed, is rather small, it nevertheless appears that the critical amplitude can be reasonably well described by an expression given by

$$A_w^* = \frac{76}{Re_D}.$$

A similar dependence of the critical amplitude on Reynolds number has been also proposed on theoretical grounds by Baggett and Trefethen (1997).

Another parameter which gives some information on the transition process, is the transition time which has already been defined above. The transition time as a function of Reynolds number and also as a function of perturbation amplitude is plotted in Figs. 5 and 6, respectively. Both figures show that the transition time decreases or transition to turbulence is faster, when the Reynolds number or the disturbance amplitude increases.

3.3. Random disturbance distribution

Next we consider the results for the random distribution of the suction/blowing through the wall according to Eq. (13) which is taken to be representative for a fully rough pipe wall. Let us first examine the results for the computation with $Re_D = 5000$ and with a root-mean-square value of RSB equal to $A_{rms} = 0.03$. The average wall shear stress is plotted as a function of time in Fig. 7. In this case we see an almost immediate increase of the wall shear stress at $t = 0$ with respect to laminar value given by Eq. (14) and subsequently a rather gradual growth. Around $t = 30$ the shear stress starts to increase towards a maximum value and this again interpreted

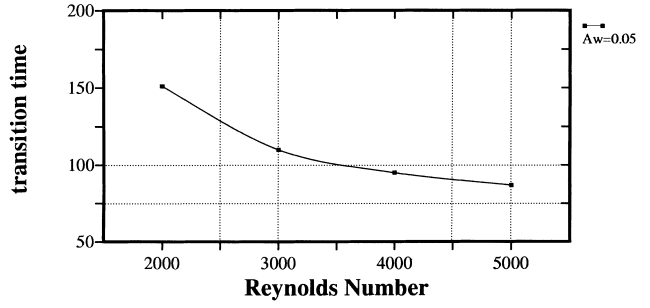

Fig. 5. Transition time vs. Reynolds number Re_D for $A_w = 0.05$.

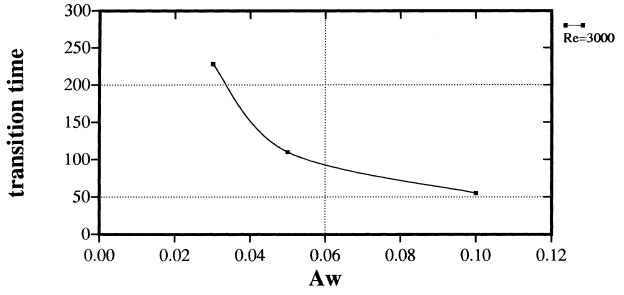

Fig. 6. Transition time vs. amplitude A_w of the PSB for $Re_D = 5000$.

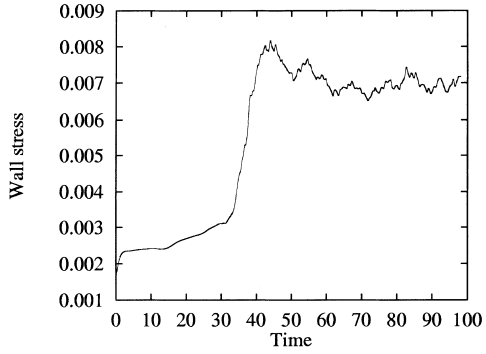

Fig. 7. Mean wall stress vs. time at $Re_D = 5000$, $A_{rms} = 0.03$.

as transition to turbulence with the time interval till the first maximum defined as the transition time.

The transition time computed according to the procedure mentioned above, is shown in Figs. 8 and 9 as function of the Reynolds number and the disturbance amplitude A_{rms}. When we compare the results shown in these two figures with Figs. 5 and 6 for the PSB case, we find that the transition time for the randomly distributed disturbance is considerable smaller than for the case of a regular disturbance. This seems to

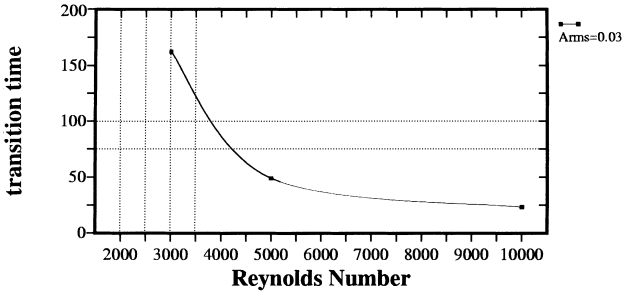

Fig. 8. Transition time vs. Reynolds number Re_D for $A_{rms} = 0.03$.

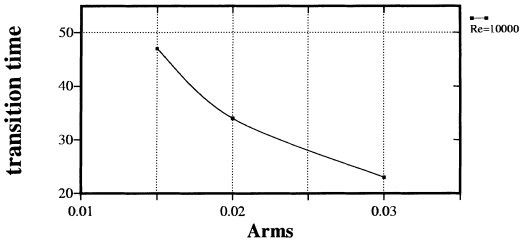

Fig. 9. Transition time vs. A_{rms} for $Re_D = 10\,000$.

agree with our intuition that transition occurs faster in a fully rough pipe.

Further results than the rather qualitative remarks made above cannot obtained from this RSB case mainly because the resolution of our computations is too small. This for instance already precludes further study of the turbulence properties of the flow after transition.

4. Conclusions

We have presented results of a direct numerical simulation of a transitional pipe flow with the objective to investigate the influence of wall disturbances on the transition from laminar to turbulent flow. The wall disturbance has been imposed by suction and blowing through the pipe wall. For the distribution of the blowing/suction we distinguish between Periodic Suction and Blowing (PSB) and Random Suction and Blowing (RSB). The blowing/suction is assumed to be representative for the effect on the flow by roughness elements on the pipe wall.

For the case of PSB the pipe flow appears to remain stable for an axisymmetric distribution of the disturbance even for a rather large amplitude of the blowing/suction. For a non-axisymmetric distribution of blowing/suction the pipe flow is unstable provided that the level of the amplitude of the blowing/suction is larger than a critical value. This critical value decreases as function of the Reynolds number according to Re^{-1}. The transition time which is approximately equal to the time period over which the effect of the disturbance on the flow grows to a level representative for a fully developed turbulent pipe flow, is found to depend on the Reynolds number and also on the amplitude of the wall disturbance.

The results for the RSB resemble those obtained for the non-axisymmetric PSB except that the disturbance seems to develop more quickly. This is borne out by a smaller transition time in comparison to the PSB case.

Acknowledgements

The first author should express sincere gratitude to the Delft University of Technology where he completed this research project with their financial support. The computer time for this project has been made available by the NCF and the TUDelft. The second author should also be grateful to TUDelft for inviting him to stay there for one month as a visiting professor joining in the collaborating research. The third author is indebted to the Tsinghua university for a visit during which this article was written. The authors are grateful to the National Natural Science Foundation of China for the support of the project.

References

Davey, A., Drazin, P.G., 1969. The stability of Poiseuille flow in a pipe. J. Fluid Mech. 36 (2), 208–218.

Davey, A., Nguyen, H.P.F., 1971. Finite-amplitude stability of pipe flow. J. Fluid Mech. 45 (4), 701–720.

Baggett, J.S., Trefethen, L.N., 1997. Low-dimensional models of subcritical transition to turbulence. Phys. Fluids 9, 1043–1053.

Bandyopadhyah, P.R., 1986. Aspects of the equilibrium puff in transitional pipe flow. J. Fluid Mech. 163, 439–458.

Eggels, J.G.M., Unger, F., Weiss, M.H., Westerweel, J., Adrian, R.J., Friedrich, R., Nieuwstadt, F.T.M., 1994. Fully developed pipe flow, a comparison between direct numerical simulation and experiment. J. Fluid Mech. 268, 175–209.

Gill, A.E., 1965. On the behaviour of small disturbances to Poiseuille flow in circular pipe. J. Fluid Mech. 21, 145–172.

Karniadakis, G.E., Israeli, M., Orszag, S.A., 1991. High-order splitting methods for the incompressible Navier–Stokes equations. J. Comput. Phys. 97, 414–443.

Lessen, M., Sadler, S.G., Liu, T.Y., 1968. Stability of pipe Poiseuille flow. Phys. Fluids 11 (7), 1404–1409.

O'Sullivan, P.L., Breuer, K.S., 1994a. Transient growth in circular pipe flow. I. Linear disturbances. Phys. Fluids 6 (11), 3643–3651.

O'Sullivan, P.L., Breuer, K.S., 1994b. Transient growth in circular pipe flow. II. Nonlinear development. Phys. Fluids 6 (11), 3652–3665.

Trefethen, L.N., Trefethen, A.E., Reddy, S.C., Driscoll, T.A., 1993. Hydrodynamic stability without eigenvalues. Science 261, 578–584.

Patera, A.T., Orszag, S.A., 1981. Finite-amplitude stability of axisymmetric pipe flow. J. Fluid Mech. 112, 467–474.

Salwen, H., Cotton, F.W., Grosch, C.E., 1980. Linear stability of Poiseuille flow in circular pipe. J. Fluid Mech. 98 (2), 273–284.

Shan, H., Zhang, Z., Nieuwstadt, F.T.M., 1998. Direct numerical simulation of a puff and slug in transitional cylindrical pipe flow. J. Fluid Mech. (Submitted).

Smith, F.T., Bodonyi, R.J., 1982. Amplitude-dependent neutral modes in Hagen-Poiseuille flow. Proc. R. Soc. Lond. A384, 463–489.